Journal of ELECTRICAL ENGINEERING, VOL 55. NO 10/S, 2004, 11-15

CHARACTERIZATION OF MAGNETO-IMPEDANCE THIN FILM MICROSTRUCTURES

I. Giouroudi*, — Hans Hauser* — G. Daalmans* — G. Rieger* — J. Wecker* ***

The magnetoimpedance (MI) effect is based on the magnetic field dependence of the transverse permeability μ of an ac current carrying conductor. Both inductance and skin effect depend on μ, thus causing a change of the impedance Z of amorphous wires, ribbons, and - at very high frequencies - also of thin films. In order to overcome this disadvantage, tri-layer structures of two 20, 50, and 100 nm thin amorphous CoFeB layers with a central 40, 100, and 200 nm thin Cu layer are rf sputtered onto a thermally oxidized Si wafer. 300 μm long strips of 3–20 μm width are structured by plasma etching and connected by ultrasonic bonding to a printed circuitboard. Magnetization curves - both of the plain film and of the structures - parallel and perpendicular with respect to the easy axis of uniaxial anisotropy are measured by the magnetooptical Kerr effect, showing an anisotropy field of 2 kA/m and low coercivity in the hard axis direction. During magnetization reversal, the domain structure in the strips was observed by Kerr microscopy, indicating possible magnetostatic coupling of the two 100 nm magnetic layers. Measurements of the frequency dependence of the complex permeability revealed ferromagnetic resonance at 1.5 GHz. The MI effect was measured by means of a network analyzer (NA), using the complex t/r ratio of the incoming (reference r) and the transmitted t wave through the sample. The NA was calibrated for linear frequency response of t at $\mu_0 Hs$ = 12 mT. The unstructured 100/200/100 trilayer (sample size 4 × 8 mm^2) showed a flat MI maximum at 65 MHz, whereas the 6 μm wide strip had a MI maximum of $(Z - Z_{Hs})/Z_{Hs}$ = 5.7% at 460 MHz with a field of $\mu_0 H$ =1.6 mT, applied by a Helmholtz coil pair, parallel to the long axis of the strip, which is oriented perpendicular to the easy axis. The MI maximum of the 50/100/50 structure strips is beyond 500 MHz. The reason of the low measured MI effect is the high contact resistance R_c =11Ohm and the inductivity L=3 nH of the 6–7 cm long leads to the strip. Measured by a four wire method, the dc resistance R_d = 4 of the 6 μm wide 100/200/100 strip is in good aggreement with the theoretical resistance of the copper layer. If directly integrated in the electronic circuit, the MI effect is increased to about 37%.

Keywords: magnetic thin film, tri-layer structure, magnetooptical Kerr effect, complex permeability

1 INTRODUCTION

Magneto-Impedance (MI) is based on the dependence of the inductivity L on the transversal ac permeability μ of a current with amplitude I and frequency $\omega = 2\pi f$ carrying ferromagnetic conductor of resistivity ρ. Due to the skin effect, which causes the current to flow near the surface of the material, reducing the effectve cross-sectional area of the material, leading to an increase in the resistive component of the impedance, the penetration depth is determined as [1]:

$$\delta = \sqrt{\frac{2\rho}{\omega \mu}} \tag{1}$$

the resistance R as well as the impedance $Z = R + j\omega L$. The MI effect is then the – usual non linear – dependence of μ on an external magnetic field H. In general, a uniaxial magnetic anisotropy with an ficive anisotropy field is induced, having the easy axis transversal to the current direction.

$$H_k = \frac{2K}{\mu_0 M_S} \tag{2}$$

M_S is the spontanious mangetization of the film.

At high frequencies only magnetization rotation occurs because the domain wall movement is strongly damped by microscopic eddy currents. Therefore, Z is minimum at H = 0, maximum at $H \approx H_k$ and minimum at $H \to \infty$. The MI ratio is defined as :

$$r_{MI} = \frac{Z_m - Z_0}{Z_0} 100\% \tag{3}$$

where Z_m is the maximum Z and Z_0 is the minimum Z at H = 0. Several hundred percent of the MI ratio have been found in amorphous CoSiB or CoFeMoSiB ribbons or wires with 10-30 μm thickness in the MHz range [2, 3, 4, 5]. The range of maximum sensitivity is shifted towards 100 MHz for 1-4 μm thick films [6]. However, these geometries are not favorable for microelectronic integration. Therefore, research on the MI effect in thin films is being done lately [7,8]. This preliminary study into this effect is to ascertain the potential use of CoFeB trilayer structured thin films for MI sensors, to correlate the magnetic properties with the impedance responses and to build up a measurement set-up with which time will be saved and more accurate results will be obtained.

2 EXPERIMENTAL ARRANGEMENT

Tri-layer structures of thin amorphous layers of CoFeB with a central copper layer were investigated (Tab. 1).

Table 1: Table of samples used for the MI measurements.

Structure (nm) CoFeB/Cu/CoFeB	Width (μm)	Length (μm)
100/200/100	4 6 10	300

* Siemens AG Erlangen, CT MM1, **Vienna University of Technology, Institute of Sensor and Actuator Systems Faculty of Electrical Engineering on Technology, Vienna of Technology, usshausstrasse 25 - 29 /366, A - 1040 Vienna, Austria, E-mail: hhauser@matwiss.isas.tuwien.ac.at

ISSN 1335-3632 © 2004 FEI STU

Amorphous cobalt rich materials are good candidates for GMI applications. They have the advantages of low magnetostriction and their magnetic anisotropy can be controlled by appropriate heat treatment. Yet, they have high resistivity. By placing a nonmagnetic elecrically conducting layer between 2 thin magnetic layers where the thickness of the magnetic layer is smaller than the core's and it's rsistivity is higher, the GMI behaviour can be improved. If permeability μ(H) is small then the impedance is determined by the resistance of the coductor and if its is large by the inductance of the magnetic layer. Theoritical investigations revealed a strong dependence of the MI effect on the strip width [3, 9]. So, the width of the strips under investigation varied while the length was constant.

The experimental setups for the calibration of the Network Analyzer, the MI frequency dependence measurements as well as the MI field dependence measurements consist of a HP Network Analyzer, Helmoltz coil with current source, a Kepko current supply and a Siemens Notebook (Fig. 1).

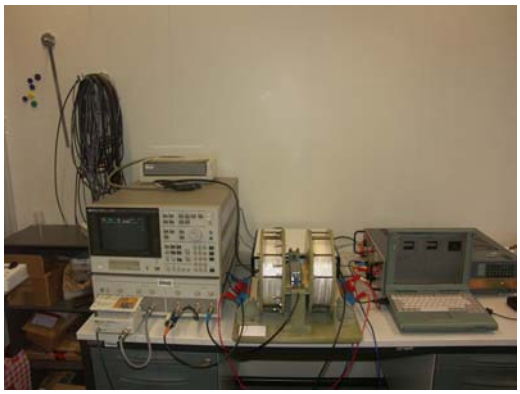

Fig. 1. Photo of the entire setup.

A LabVIEW program was used in order to calculate the frequency dependence of the strip impedance. The calculation of the real and imaginary parts of the strip impedance is automatically done using equation (1):

$$Z = Z_l\left(\frac{2}{T} - 1\right) \tag{4}$$

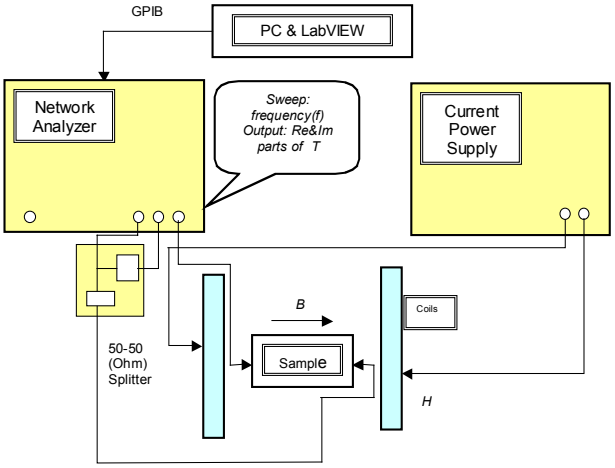

Fig. 2. Block diagram of the setup used for calibration of the Network Analyzer as well as for the MI frequency dependence

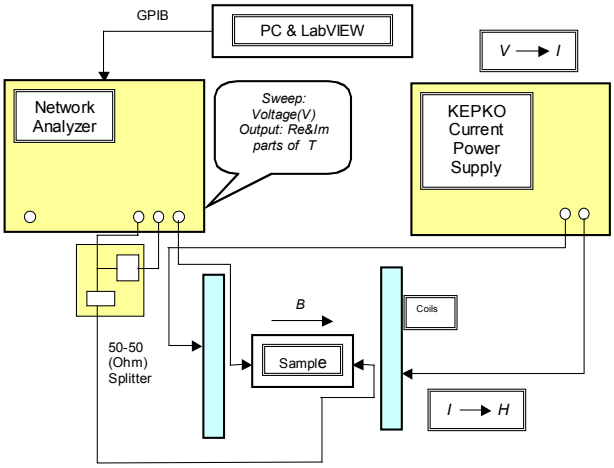

Fig. 3. Block diagram of the setup used for the MI field dependence

Specifically, the real and imaginary parts of the transmitted waveT are acquired from the Network Analyzer and then replaced at equation (4). Zl is the known output impedance (50 Ohm). The block diagram of this set-up is presented if Figure 2.

The applied frequency varied from 10 MHz to 500MHz. The Network Analyzer with the sample connected has been calibrated for each measurement at 15mT. Then a measurement for each strip of each sample was carried out at zero field, μoH = 0, and at an applied field of $\mu_0 H$ = 1.6 mT, in order to determine the frequency where the maximum rMI occurs. The field dependent MI measurements are then carried out at this frequency. A LabVIEW program was used to determine the MI ratio in response to the applied field *B*. A DC bias voltage, acquired from the Network Analyzer, was sent to a KEPKO current source which was used for applying the external field to the sample. The block diagram of this set-up is shown in Figure 3.

The external field varied from –15 mT to 15 mT and backwards (15 mT to –15 mT) with a stepwidth of 0.5 mT. The MI ratio was automatically calculated using equation (2):

$$r_{MI} = \frac{\sqrt{T_{\mathrm{Re}}^{\,2}\left(2 - T_{\mathrm{Re}}^{\,2}\right) + T_{\mathrm{Im}}^{\,2}\left(2 + T_{\mathrm{Im}}^{\,2}\right)}}{T_{\mathrm{Re}}^{\,2} - T_{\mathrm{Im}}^{\,2}} - 1 \tag{5}$$

Specifically, the real and imaginary parts of the transmitted wave T are acquired from the Network Analyzer and replaced at equation (5). A closer measurement from –5 mT to 5 mT and backwards (5 mT to –5 mT) with a stepwidth of 0.05 mT was also carried out for each strip of each sample.

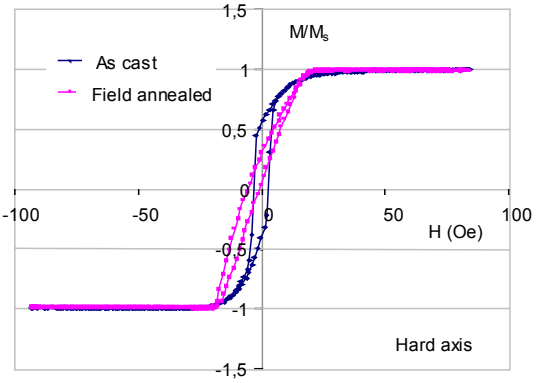

Fig. 4. Magnetization in arbitrary units versus field parallel to H_a. of the 100/200/100nm unstructured tri-layer, before and after annealing.

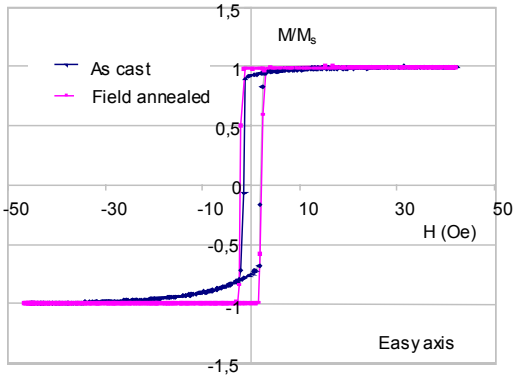

Fig. 5. Magnetization in arbitrary units versus field parallel to *ea* of the 100/200/100nm unstructured tri-layer, before and after annealing.

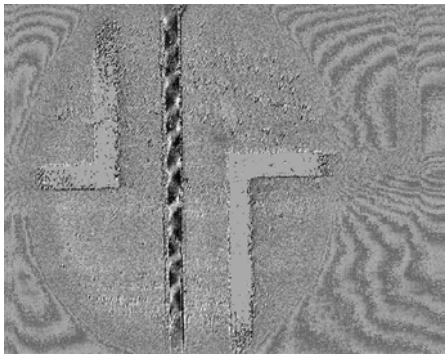

Fig. 6. Magnetization in arbitrary units versus field parallel to H_a of the 100/200/100nm unstructured tri-layer, before and after annealing.

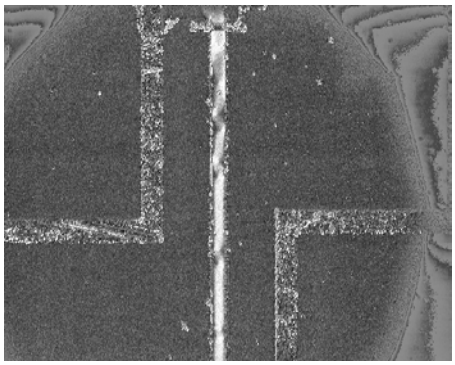

Fig. 7. Magnetization in arbitrary units versus field parallel to *ea* of the 100/200/100nm unstructured tri-layer, before and after annealing.

4 RESULTS AND CONCLUSIONS

The magnetization curves of the films were measured using the magneto-optical longitudinal Kerr effect (MOKE). Specifically, a polarized light beam, reflected from the sample surface, experiences a rotation of its polarization plane depending on the magnetization direction with respect to the projection of the reflected light direction in the film plane. By means of an analyzer and a photo-detector this is evaluated into a voltage signal. The field was applied by means of a permanent magnet with a core inside, which can provide fields up to almost 3000Oe. The hysteresis loops for the 100/200/100 nm tri-layer were obtained before and after annealing parallel to the easy and hard axis. It reveals an anisotropy field of 1.6kA/m parallel to the hard axis (Figure 4,5).

The domain structure of the 100/200/100 nm tri-layer was observed using a Kerr effect microscope arrangement. This observation in reflection is based on small rotations of the polarization plane of the light and become visible in a polarizing microscope. The non-magnetic background image is digitally subtracted and the magnetic contrast is enhanced by averaging and electronic manipulation [10].

Figure 6 shows the magnetization before annealing in the strip of 10μm with l transverse to the easy axis and the Figure 7 after annealing. The annealing was carried out at 280oC, for 30 min. at a field of 320 kA/m applied perpendicular to the strip. The samples were cooled down in field. As observed, the magnetization appears to nearly align along the length of the strip (after field annealing) thus having an easy axis along the longitudinal direction. This could possibly be attributed to the fact that a shape anisotropy is created which tries to align the moments along the length of the strip. Since no other agent is present to oppose to this during the heat treatment, an easy axis along the length of the strip is created. On the contrary, before field annealing the domain structure of the as cast samples is nearly perpendicular to the long axis.

In Figures 8 and 9 for the 100/200/100 nm tri-layer, the results of the 4, 6 and 10 μm strips impedance dependence over frequency as well as of the MI field dependence, before and after annealing, are presented.

Before annealing a double peak occurred but after that it seems that the magnetizations have rotated thus causing a longitudinal magnetic anisotropy and a single peak when MI is being measured. In order to obtain more accurate results and to save time, the whole set-up has been automated. Several LabVIEW programs have been created in order to obtain the results automatically. Double peak GMI curves and MI maximums around 4% have been obtained for several samples.

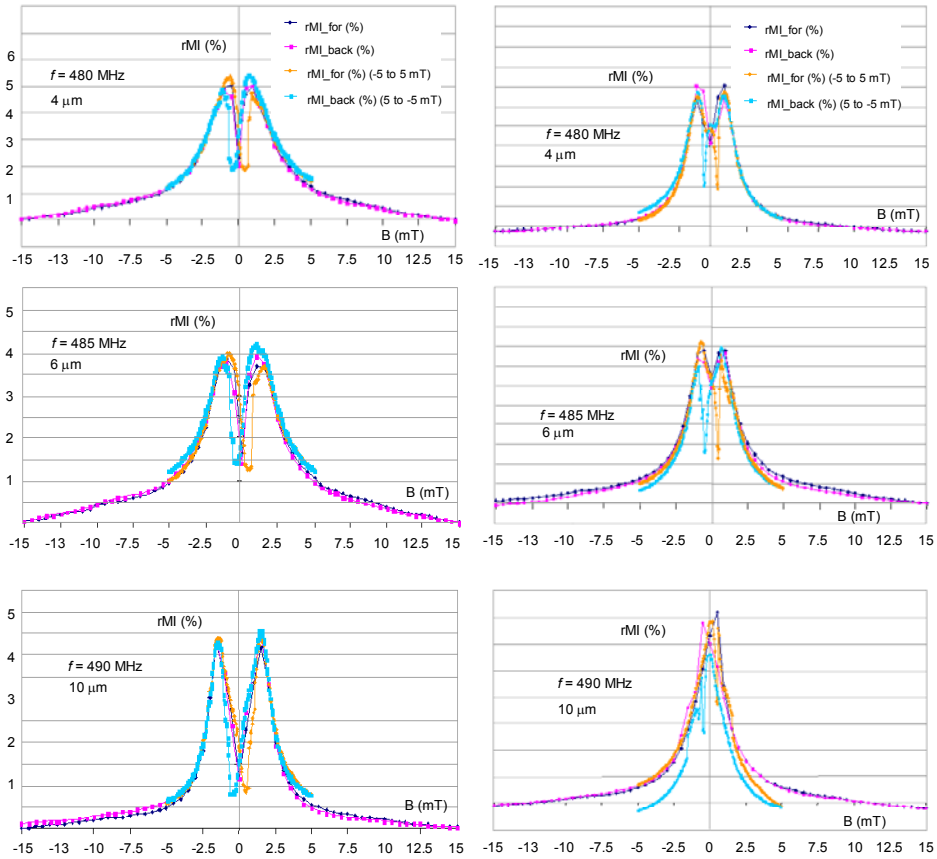

Fig. 8. Results of the strips impedance dependence over frequency of the 100/200/100 nm tri-layer, before (left column) and after (right column) annealing at 280°C, 30 min in a field of 4.9 kOe.

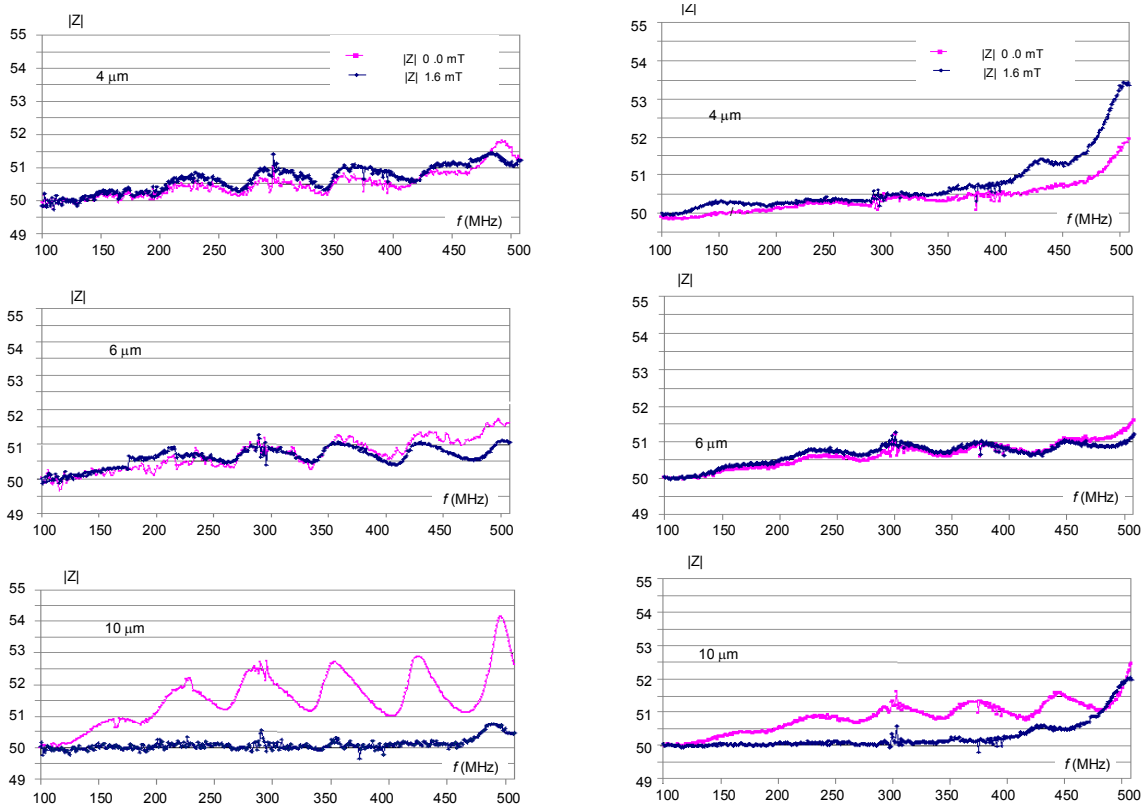

Fig. 9. Results of the MI field dependence of the 100/200/100 nm trilayer, before (left column) and after (right column) annealing.

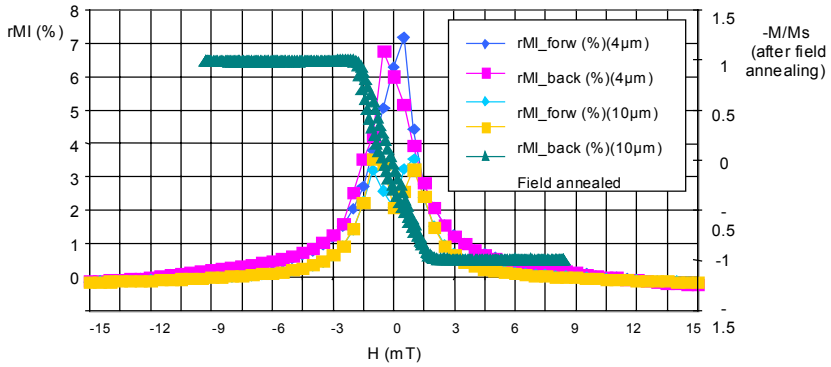

Fig. 10. MI response of 10μm strip (100/200/100 nm trilayer) along with its corresponding hard axis hysteresis loop, before field annealing

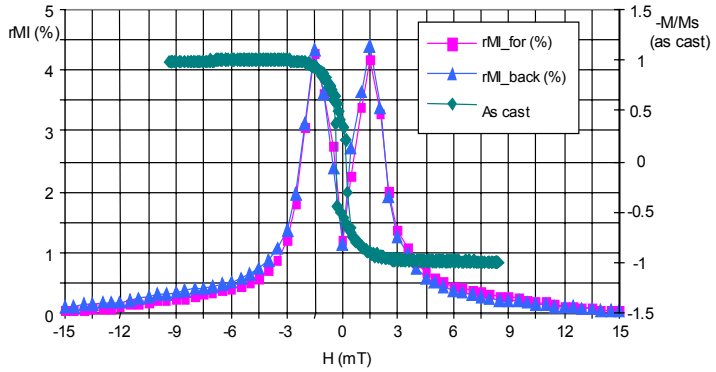

Fig. 11.. MI response of 4 and 10μm strips (100/200/100 nm trilayer) along with its corresponding hard axis hysteresis loop, after field annealing

In Figure 10 the MI response of the 100/200/100 nm trilayer, 10 μm strip along with its corresponding hard axis hysteresis loop is shown, before field annealing. The MI peaks appear to coincide with the anisotropy field obtained from the hysteresis loop. It is estimated by this, that during formation of the films the anisotropy had been set nearly transverse therefore a double peak GMI curve is obtained. By annealing the samples though the shape anisotropy overules the magnetic anisotropy. Therefore magnetization is aligned along the length of the strip instead of perpendicular.

The MI response of the 100/200/100 nm trilayer, 4μm and 10 μm strip along with its corresponding hard axis hysteresis loop is shown in Figure 11, after field annealing. As observed for the widest strip (10μm) the MI peaks appear to coincide with the anisotropy field obtained from the hysteresis loop while for the 4 μm a single peak GMI curve is obtained due to longitudinal anisotropy. This is in agreement to previous theoritical investigations that revealed a strong dependence of the MI effect on the strip width b. As the strip becomes wider and the length remains the same, the shape anisotropy is weakened. This way it is easier to set the magnetic anisotropy perpendicular to the length of the strip [9,10].

The work that could be done in the nearest future concerns the investigation of wider strips as well as the further investigation of 20/40/20 nm and 507100/50 nm trilayers. Finally the annealing conditions for setting the anisotropy should be developed

Acknowledgement

The authors would like to express their gratitude to Siemens AG, Corporate Technology, Materials and Manufacturing 1, Innovative Electronics, in Erlangen, Germany. They acknowledge as well the financial suport from the FWF Project 16698-N02.

REFERENCES

[1]. H. Hauser, L. Kraus, P. Ripka, "Giant Magnetoimpedance Sensors", IEEE Instr.&Meas. Mag. (June 2001) 28-32.

[2]. L. V. Panina et al., IEEE Trans. Magn. 31 (1995) 1249.

[3]. L. V. Panina et al., J. Appl. Phys. 89 (2001) 7221.

[4]. J. M. Barandiaran et al., IEEE Trans. Magn. 38 (2002) 3051.

[5]. G. V. Kurlyandskaya et al., Appl. Phys. Lett. 82 (2003) 3053.

[6]. T. Uchiyama et al., IEEE Trans. Magn. 31 (1995) 3182.

[7]. T. Morikawa, Y. Nishibe, H. Yamadera, Y. Nonomura, M. Takeuhci, Y. Taga, "Giant magnetoimpedance effect in layered thin films", IEEE Trans. Magn. (1997) 4367.

[8]. L. V. Panina, K. Mohri, K. Bushida, M. Noda, "Giant magnetoimpedance and magnetoinductive effects in amorphous alloys", J. Appl. Phys. (1996) 6198.

[9]. A. Gromov et al., IEEE Trans. Magn. 34 (1998) 1246.

[10]. A. Hubert, R. Schäfer, "Magnetic Domains", Berlin, Springer (1998).

Received 28 June 2004